Effects of Collision Velocity and Mirror Ratio on Collision/Merging Processes of Field-Reversed Configurations*)

Daisuke HARASHIMA, Tomohiko ASAI, Daichi KOBAYASHI, Taichi SEKI, Tatsuhiro WATANABE and Tsutomu TAKAHASHI

Department of Physics, College of Science and Technology, Nihon University, Tokyo 101-8308, Japan

(Received 10 January 2022 / Accepted 15 March 2022)

The effects of collision velocity and mirror ratio on the collision/merging processes of field-reversed configurations (FRCs) were experimentally evaluated. In the collisional merging experiment, the reversal field structure is reformed despite experiencing destructive perturbations resulting from collisions at supersonic/Alfvénic velocity. However, reformation of the reversal field structure was not observed under some experimental conditions, such as slow collision velocity or low mirror ratio. The radial profile of the reversal field structure and its time evolution were observed using an internal magnetic probe array. Collisional merging of FRCs was attempted by adjusting the external field profile. Experimental results suggest the dependence of the trapped poloidal flux of the formed FRC after merging on collision velocity and external magnetic boundary.

Keywords: field-reversed configuration, collisional merging, mirror ratio, collision velocity

DOI: 10.1585/pfr.17.2402056

1. Introduction

An field-reversed configuration (FRC) is a high-beta compact torus with a predominantly poloidal magnetic field generated by toroidal plasma current [1, 2].

The collisional merging formation experiment of FRCs has been conducted in the FRC Amplification via Translation Collisional Merging (FAT-CM) device [3]. In this experiment, the initially-formed plasmoids with an FRC-like reversal magnetic structure are formed in two separate formation regions. Each plasmoid is translated along the magnetic pressure gradient into the middle of the confinement chamber immersed in the external field and then collide at supersonic/Alfvénic velocity [4]. In the collision/merging processes, the initial-plasmoids lose their reversal magnetic field structure, which is characteristic of an FRC. Despite the plasmoids experiencing such a destructive perturbation, the reversal magnetic field structure is reformed at the quiescent equilibrium phase after merging [5]. However, this reformation of the reversal magnetic field structure was not observed under some experimental conditions. The experimental observation and two-dimensional (2-D) resistive magnetohydrodynamics (MHD) simulations suggest the applied mirror magnetic field in the confinement region is the key condition of the reformation process [6, 7]. The axial magnetic profile, such as the mirror ratio, may change the collision velocity (relative velocity of two plasmoids at the collision). The effects of collision velocity changes on the reformation process should also be examined.

In this paper, the effects of collision velocity and the mirror ratio on the reversal magnetic structure reformation process were evaluated experimentally.

2. Experimental Device

Figure 1 shows a schematic diagram of the FAT-CM device and the axial profile of the external field. This device has a confinement region in the center and field-reversed theta-pinch type formation regions at both ends. The formation region consists of a quartz tube and theta-pinch coils are situated around it. The theta-pinch coils are arranged in a conical configuration to produce a magnetic pressure gradient for the acceleration and translation of initial plasmoids. The confinement region consists of a cylindrical metal chamber in the center and conical chambers at both ends. The mirror/straight coils are placed coaxially on the outside of the chamber to provide the external field (~0.06 T) able to sustain the FRC after merging. The rise and decay times of the current on the mirror/straight coil are several tens or hundreds of milliseconds, which are much longer than typical energy confinement times (around ~140 μs) of the FRC formed by the collisional merging method. Also, an internal magnetic probe array used to observe the radial profile and its time evolution of the internal magnetic structure during the collisional merging processes was installed in the center of the confinement region, as shown in Fig. 2 [8].

3. Experimental Setup

3.1 Adjustable axial external field profile

The axial profile of the external field was adjusted by

author's e-mail: asai.tomohiko@nihon-u.ac.jp

*) This article is based on the presentation at the 30th International Toki Conference on Plasma and Fusion Research (ITC30).

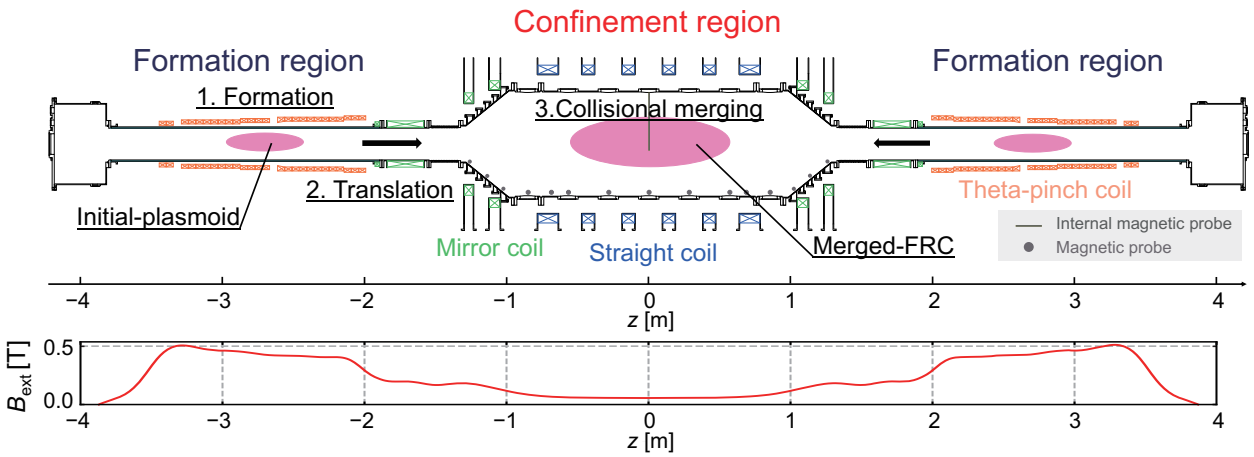

Fig. 1 Schematic diagram of the FAT-CM device and axial profile of the external field.

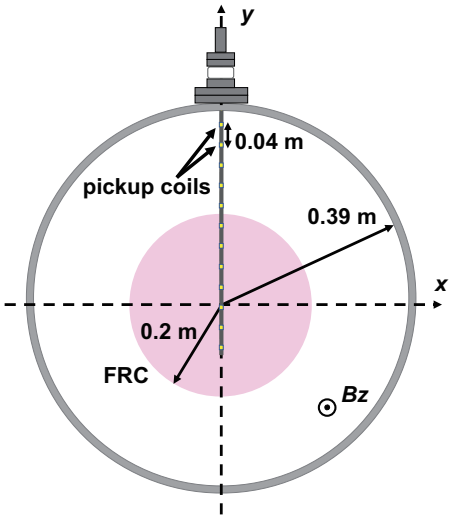

Fig. 2 Illustration of a cross-sectional view of the installed probe in the mid-plane of the FAT-CM device.

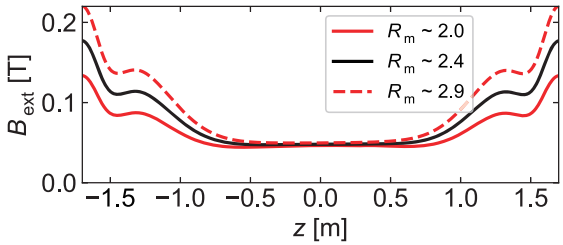

Fig. 3 Axial profile of the external field with three different mirror conditions.

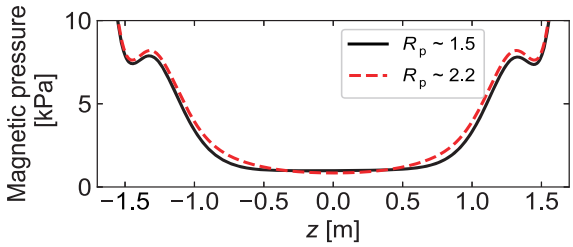

Fig. 4 Axial profile of the magnetic pressure (R_p ~ 1.5 and R_p ~ 2.2, respectively).

the current applied to the confinement coil and/or the number of turns. The mirror ratio R_m in the standard case was around 2.4. In cases 1 and 2, the mirror ratio was varied by changing the current driven on the mirror coil. The mirror ratios in cases 1 and 2 were around 2.0 and 2.9, respectively, as shown in Fig. 3. The change in R_m determines the length of the confinement region of the colliding FRCs, which shortens as R_m increases. It may also have an effect on the reformation process of FRC.

In case 3, the straight field structure was changed by increasing the number of turns at both ends of the straight coils, as shown in Fig. 4. Here the ratio of the external magnetic pressure $B_{ext}^2/2\mu_o$ at $z = \pm 0.75$ m to the midplane ($z = 0$) is defined as R_p. In the standard case, R_p is approximately 1.5. Case 3 is the maximum case R_p (~2.2) in the current experimental device setup. Thereby, the distance between the mirrors was shortened with respect to the FRC separatrix length, and the axial magnetic pressure gradient was increased. The change in the shape of the confinement field from a mirror shape with a flat center to a convex mirror shape is also expected to have an effect on the reformation process.

3.2 Dependence of collision velocity on external field profile

Collision velocity is determined by the difference in magnetic pressure gradient structure between the formation ($z = \pm 3$ m) and confinement ($z = 0$) regions [9]. Figure 5 shows the dependence of the collision velocity in each case. Here, the translation velocity of the plasmoids was estimated using the time-of-flight method with the signal from the magnetic probe arranged along the wall of the vacuum chamber in the confinement region. In case

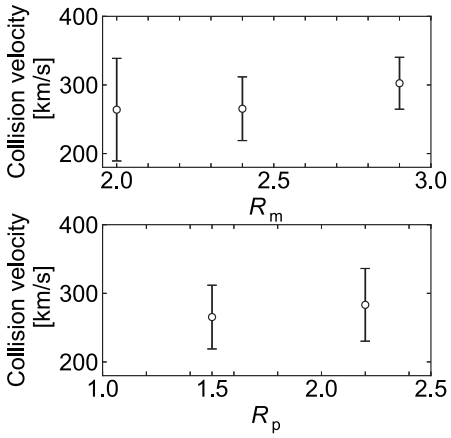

Fig. 5 Collision velocity dependence on the axial profile of the external field.

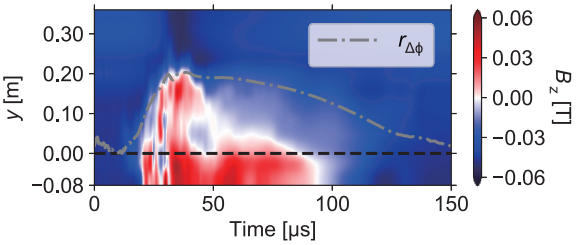

Fig. 6 Typical contour map of the B_z radial profile as a function of time in collisional-merging FRC plasma.

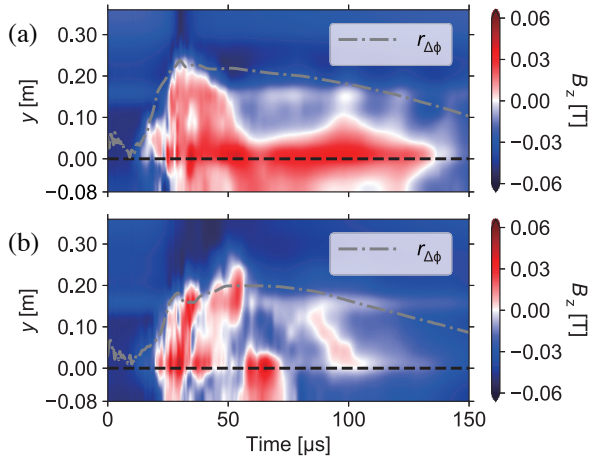

Fig. 7 Contour maps of the B_z radial profile as a function of time for mirror conditions of $R_m \sim 2.0$ ((a) Reformed case, (b) Non reformed case).

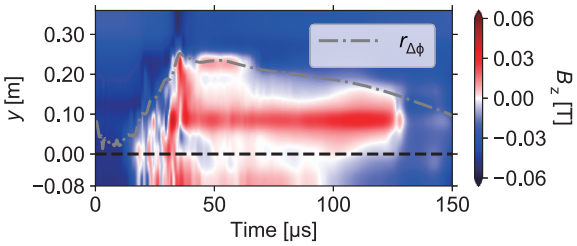

Fig. 8 Contour map of the B_z radial profile as a function of time for mirror conditions of $R_m \sim 2.9$.

1, which is a smaller R_m case, the average collision velocity was unchanged compared to the standard case. On the other hand, case 2 showed a 14% increase. In case 3, the average collision velocity was increased by ~7%. However, no significant increase was not observed for the standard deviations. So, the effects of changes in the external field profile and collision velocity can be discussed independently.

4. Experimental Results

4.1 Typical collisional merging process of FRC

Initial-plasmoids were generated using deuterium gas. The typical averaged electron density of the initial-plasmoids and merged-FRC were $\sim 10^{21}$ m^{-3} and $\sim 10^{20}$ m^{-3}, respectively. Figure 6 shows a typical contour map of B_z radial profile as a function of time in the collisional merging process of FRC plasma, observed by the internal magnetic probe array. The dashed-dotted line denotes the excluded flux radius $r_{\Delta\phi}$ at the midplane, where $r_{\Delta\phi}$ is approximately equal to the separatrix radius r_s. A typical $r_{\Delta\phi}$ of merged-FRC is ~0.2 m. The perturbing magnetic field was observed during the collision phase ($t \sim 20$ - 40 μs). After relaxation ($t \sim 70$ μs), also termed the quiescent equilibrium phase, the FRC-like reversal magnetic structure was clearly observed. After that, the trapped poloidal flux and excluded flux radius decayed and became almost zero at $t \sim 150$ μs. Note that the inserting internal magnetic probe array affects the performance of FRC. An FRC can move radially because of its simply connected geometry. In some shots, it seems that the position of the FRC after merging was shifted or the internal structure was axisymmetric. This may be due to the FRC's own motion and invasive effect of the internal magnetic probe array. Also, the configuration lifetime of the plasma was shortened from ~250 μs to ~150 μs by inserting the internal magnetic probe array.

4.2 Dependence of mirror ratio

4.2.1 Dependence on the mirror field structure

Figure 7 shows contour maps of the B_z radial profile as a function of time for mirror conditions of $R_m \sim 2.0$ and Fig. 8 is for R_m ~2.9. The FRC-like reversal magnetic structure was observed as the mirror ratio was decreased or increased, as shown in Figs. 7 (a) and 8. However, there are some shots where the reversal field is not reformed, as shown in Fig. 7 (b). Non-reformed shots refer to the non-observation of the reversal field or that the formation time is clearly shorter than the reformation shots. The probability of the reformation of the reversal magnetic structure in all shots that were successfully translated and merged for smaller and larger R_m cases were ~80% and ~50%, re-

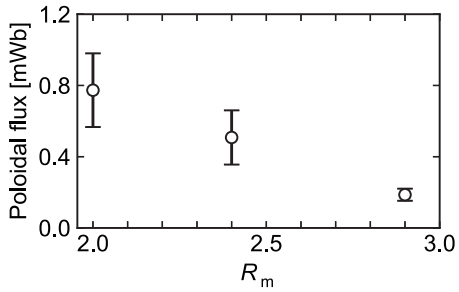

Fig. 9 Comparison of the poloidal flux measured using an internal magnetic probe array ($R_m \sim 2.0$, ~ 2.4 and ~ 2.9, respectively).

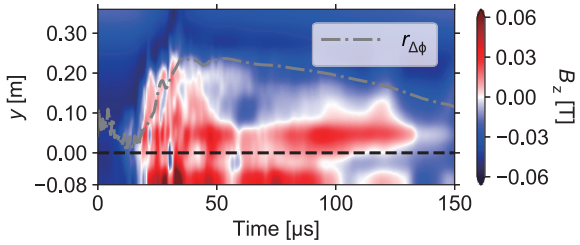

Fig. 10 Contour map of the B_z radial profile as a function of time for mirror conditions of $R_p \sim 2.2$.

spectively. The probability of reformation in the standard case was ~53%. Figure 9 shows the poloidal flux estimated from the B_z radial profile at the time when the reversal field is reformed, and the radial profile of data points was fitted by the rigid rotor model [1,2], and the fitting curve was integrated in the radial direction to estimate the poloidal flux. The poloidal flux can be estimated by

$$\phi = -\int_0^R 2\pi r B_z dr = \int_R^{r_s} 2\pi r B_z dr, \quad (1)$$

where R is the radius of the magnetic axis ($B_z = 0$), and r_s is the separatrix radius of the FRC. As shown in Fig. 9, the poloidal flux decreased with increasing mirror ratio. These results suggest that a too strong mirror field will prevent FRC merging.

4.2.2 Dependence on the straight field structure

Contour map of the B_z radial profile as a function of time for mirror condition of $R_p \sim 2.2$ is shown in Fig. 10. An FRC-like reversal magnetic structure was also observed in case 3, as shown in Fig. 10. The probability of the reformation was ~64%. As shown in Fig. 11, the poloidal flux was unchanged in this case. The comparison of shape parameters of the formed FRC plasma in each case is listed in Table 1. The values in Table 1 denote the average value and standard deviation, respectively. Here, the full width at half maximum value of the axial profile of the excluded flux radius is defined as the separatrix length $L_{\Delta\phi}$. Also, the plasma volume $V_{\Delta\phi}$ is defined as the volume of the body rotated around the z-axis in the region enclosed by the axial profile of the excluded flux radius between the length. In case 3, the separatrix length was shorter, and the volume was smaller than that of the standard case. Figure 12 shows a time slice of the axial profile of the excluded flux radius at the quiescent equilibrium phase. The plots and error bars denote the moving averages and standard deviations in the time series between 55.5 - 85.5 μs, respectively. The two-peaked or flat shape of the merged-FRC was occasionally observed in the standard case, whereas the two-peaked and flat shapes were not observed in case 3. The typical magnetic structure in the two-peaked shape case is shown in Fig. 13. This structure cannot be said to be a clear FRC-like structure. The axial profile of the external field in the confinement region has a sufficient effect on the reformation process of FRC and the shape of the formed FRC after merging. The elongation of an FRC is related to the stability of tilt mode [2]. Therefore, the axial profile of the external field is important when forming a more stable

Table 1 Typical shape parameters of formed FRC (w/probe).

R_p	$r_{\Delta\phi}$ [m]	$L_{\Delta\phi}$ [m]	$V_{\Delta\phi}$ [m^3]
1.5	0.19±0.01	1.9±0.1	0.16±0.01
2.2	0.21±0.01	1.3±0.1	0.14±0.01

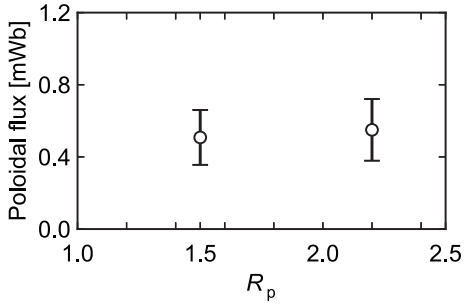

Fig. 11 Comparison of the poloidal flux measured using internal magnetic probe array ($R_p \sim 1.5$ and $R_p \sim 2.2$, respectively).

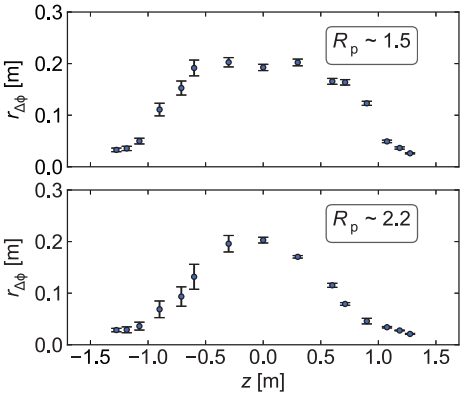

Fig. 12 Time slice of the axial profile of the plasma radius (w/probe).

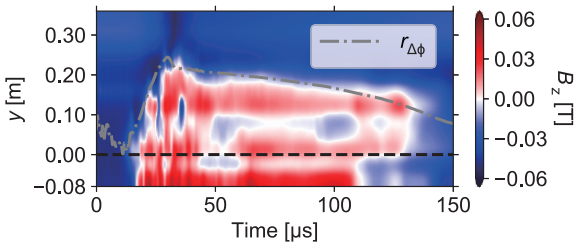

Fig. 13 Contour map of the B_z radial profile as a function of time for $R_p \sim 1.5$ when two peaks are observed.

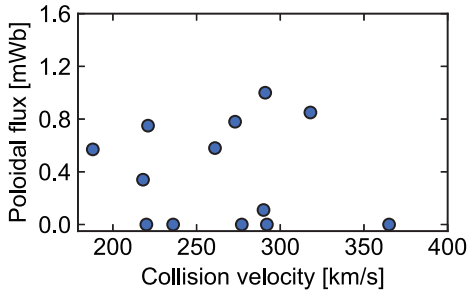

Fig. 14 Dependence of poloidal flux measured using an internal magnetic probe array on the collision velocity.

FRC in collisional merging.

4.3 Dependence of collision velocity

Figure 14 shows the dependence of the estimated poloidal flux on the collision velocity in the standard case ($R_m \sim 2.4$ and $R_p \sim 1.5$). The collision velocity slightly varies shot-by-shot, which is due to the dispersion. The shots where the reversal magnetic structure was not reformed are plotted as zero. A positive correlation between the trapped poloidal flux of the formed FRC and the collision velocity is suggested. Also, the poloidal flux increased depending on the translation velocity in the 2-D resistive MHD simulation [9]. This experimental result is viewed as approximately consistent with simulation results.

5. Summary

The effects of collision velocity and mirror ratio on the collision/merging processes of FRC were experimentally evaluated. As predicted by MHD simulation, a positive correlation between FRC performance and collision velocity was observed in the experiments. The trapped poloidal flux decreased with increasing mirror ratio R_m. Especially in the case of increasing R_p, the two-peaked shape of the merged-FRC, which is sporadically observed in the standard case, was not observed. These experimental results suggest that the performance and stability of collisional merging formed FRC strongly depend on the collision velocity and external magnetic boundary.

Acknowledgments

The authors would like to acknowledge all members of the Fusion Plasma group, Nihon University. This work was partially supported by JSPS KAKENHI Grants Number JP19K21868, 20H00143 and Nihon University, College of Science and Technology, Grant for Project Research.

[1] M. Tuszewski, Nucl. Fusion **28**, 2033 (1988).
[2] L.C. Steinhauer, Phys. Plasmas **18**, 070501 (2011).
[3] T. Asai *et al.*, Nucl. Fusion **59**, 056024 (2019).
[4] D. Kobayashi *et al.*, Phys. Plasmas **28**, 022101 (2021).
[5] T. Asai *et al.*, Nucl. Fusion **61**, 092036 (2021).
[6] H. Gota *et al.*, Rev. Sci. Instrum. **89**, 10J114 (2018).
[7] F. Tanaka *et al.*, Plasma Fusion Res. **13**, 3402098 (2018).
[8] T. Watanabe *et al.*, Rev. Sci. Instrum. **92**, 053541 (2021).
[9] D. Kobayashi *et al.*, Plasma Fusion Res. **15**, 2402020 (2020).